Efficient 3D and 2D Failure Conditions for UD Laminae and their Application within the Verification of the Laminate Design

R. G. Cuntze
formerly with MAN Technologie AG, Augsburg, Germany;
D-85229 Markt Indersdorf, Tel & FAX: 0049 8136 7754, E-mail: Ralf_Cuntze@t-online.de.

Keywords: Static failure criteria, UD laminae, reserve factors E 258

Abstract:

The paper presents a set of three-dimensional (3D) and 2D strength failure conditions for unidirectional (UD) laminae made from fibre-reinforced plastics (FRP). The conditions are based on a concept termed the Failure Mode Concept (FMC) which provides failure conditions formulated on UD lamina level that allows for a prediction of the critical lamina failure mode, and finally of laminate failure. Following the FMC there are five independent conditions: for Inter Fibre Failure (IFF) three and for fibre failure (FF) two conditions. These are based on averaged lamina stresses. The IFF conditions were basically developed in 1996 and later contributed [1, 2] to a 'World-Wide Failure Exercise (WWFE) on failure theories', Ref [3].

In this paper a single but effective modification of one IFF condition is highlighted. It consists in the replacement of the 'shear mode IFF 2' by a numerically advantageous simplified formulation for the 3D and for the 2D case. A very satisfying verification of the 3D IFF2 condition , reduced to 2D, as well as for a directly formulated 2D IFF2 condition has been achieved when judging them versus the 2D experiments provided by the WWFE and other sources.

As *design verification* demands for an accurate determination of the reserve factor its determination is presented for both the linear and the non-linear case. Values are given for one example.

1. Introduction

Design verification requires "No relevant *limit state* of a failure mode is exceeded in any *dimensioning load case*". In order to faster meet this requirement industry seeks to replace the expensive 'Make and Test' design method by verified and benchmarked predictive tools that engineers may use with confidence. Practical composite failure conditions for UD laminae are amongst these design tools.

Designers tend to carry out refined stress analyses, but then, they are forced to assess multi-axial stress states with failure conditions that may have shortcomings or are not verified by a sufficient amount of experimental data. This data is based on specimens that represent so-called isolated UD laminae. In this paper, as failure conditions 3D and 2D-UD IFF conditions are investigated. Emphasis is put on the shear failure mode IFF2 the former formulation of which numerically is not

practical enough. As failure conditions for a lamina -utilized as building block of a *laminate*- do not fully cover the *failure behaviour of the embedded laminae*, failure theories are to be addressed that consist, of both, of the failure conditions itself and of non-linear analysis to consider the degrading lamina's behaviour within the laminate. Applying this, an accurate input for the computation of the design assessing reserve factor is provided.

Since 1992 a World-Wide Failure Exercise [4-6] is underway to monitor and check the current capability of methods for predicting the strength of fibre composite laminates. It was organised at UMIST and QinetiQ, UK, by Prof. Dr. M. J. Hinton, Mr. P. D. Soden and Dr. A. S. Kaddour. In this exercise test cases were selected to challenge the theories to the full. These test cases include carbon and glass fibres, different epoxy matrices, stacking sequences, and loading conditions involving uni-axial and bi-axial tension and compression, torsion shear, as well as combinations of them. As test results, those available from tube specimens were chosen because the simpler coupon specimens are encountered with the free edge effect. Also, a wider range of stress states can be applied to tubes by combinations of internal or external pressure, torsion, and axial load, see Ref [6]. Nevertheless some problems remain. The tubes have to be designed in order: to avoid torsion and compression buckling, to avoid failures at the end constraints, and to minimise possible changes in geometry (widening, barrelling). The usually given fracture stress states or –in other words- multi-axial strengths are calculated on basis of *un-deformed* tube dimensions with no allowance made for shape change during loading.

When predicting laminate behaviour, which is not the objective of this paper, it is to mention: Test results from *isolated* UD lamina specimens such as a tensile coupon are load-controlled. They are results of weakest link type whereas the in-situ behaviour of an *embedded* lamina is strain-controlled and therefore of redundant type [2]. This fact shows up that a good mapping of the course of 'isolated UD test data' does not represent the full information necessary for laminate analysis.

Generally, and not restricted to the WWFE, there is a lack of real 3D UD tests. Further, data are even missing in some domains of the provided 2D test cases. Therefore, the 3D UD failure conditions can only be partly verified but the 2D ones can, sometimes only after re-evaluation of the test data of the provided test case. Both, the measurement of test results as well as the evaluation of test results may involve errors, which is to be considered when verifying failure models.

For design engineers the choice of the macro-mechanical level in modelling is mandatory because they receive as input macro-mechanical stresses from *stress* analysis. Hence the *strength* analysis, delivering the *design verification,* can be carried out on the same level on the macro-mechanical level. But one has to keep in mind: Describing failure by macro-mechanical stresses is different to

describing failure by the really failure mechanisms-causing micro-mechanical stresses and, this is not always directly possible such as is later delineated for fibre failure under tension (FF1).

In any static design, dependent on the actual design requirements, a designer~~in general~~ in general has to dimension a laminate against two types of failure,~~;~~ namely~~:~~ *initial failure* and *final failure*~~which is to be dedicated to the *laminate*. with its loads at fracture level demands for an analysis beyond IFF.~~

An IFF mode normally indicates the *initial failure* or *onset of failure* in a laminate whereas the appearance of a FF mode in a single *lamina* ~~embedded in a laminate~~usually marks the *final failure* of the~~at~~ laminate. Also fracture critical may be the so-called wedge failure mode IFF3, [7, 2]. In the case of brittle FRP composites failure coincides with fracture.

At the end of a design campaign the designer has to predict reliable reserve factors. In order to give a guideline, how to achieve the desired *design verification* by demonstrating positive Margins of Safety *MS* or reserve factors larger than one (f_{Res} = *MS* + *1)*, the determination of accurate reserve factors is depicted. In this context, the designer has to tackle the determination of f_{Res} for linearly and non-linearly behaving laminae and laminates, and further has to keep in mind: Verified failure conditions, alone, are just one part to achieve the demanded result 'reliable reserve factors'.

The two aims of this paper are: 1) the development of a numerically simple set of failure conditions with showing there is no loss in mapping quality, and 2) the derivation of associated reserve factors for linear as well non-linear strength analysis. The value of this work lies in the simplification of the shear mode condition IFF 2 and the presentation of reserve factor formulations in order to achieve the *design verification* which is a precondition for product certification.

2 Basics

~~□~~2.1 Lamina Stresses, Invariants, and Properties

The characterisation of the strength of transversally-isotropic composites requires the measurement of five independent basic lamina strengths: $R_{\parallel}^{t}$ and $R_{\parallel}^{c}$ (tensile and compression strengths parallel to the fibres); $R_{\perp}^{t}$ and $R_{\perp}^{c}$ (tensile strength and compressive strength transversal to the fibre direction); and $R_{\perp\parallel}$ (~~fibre parallel~~ shear strength transverse/parallel to the fibres). The measurement of just these *5* strengths is standard.

Fig. 1 depicts the 3D stress state $\{\sigma\} = (\sigma_1, \sigma_2, \sigma_3, \tau_{23}, \tau_{31}, \tau_{21})^T$. For completeness and general understanding it further depicts the 5 strengths in symbolic denotation, applied in the German guideline VDI 2014 [8] to avoid misunderstanding in the application of material properties (in

brackets the US denotation), and the 5 elasticity quantities of a UD material element. **Fig. 2** demonstrates a 2D stress state of a lamina in a laminate.

2.2 Failure Modes: FF Modes and IFF Modes

From viewing fractography images of UD material it can be concluded what is delineated in **Fig. 3:**

- The total number of fracture mode[14]s [1 ,2 ,9, 10] is five: two FF modes and three IFF modes. The IFF modes incorporate cohesive fracture of the matrix and adhesive fracture of the fibre-matrix interface. Both fracture types are often termed~~as~~ 'matrix failure'.
- Two of the 3 IFF modes, IFF1 and IFF2, may be tolerated if the design requirements allow for.
- Like the fibre failure modes FF1 and FF2 the 'explosive' effect of the so-called *wedge fracture* failure IFF3 ~~(which is an IFF mode caused by the transverse stress a $\sigma_{\perp}^{c}$ caused IFF)~~ of a lamina in a laminate, which is an IFF mode caused by high transverse compressive stress σ_3^c~~described in~~, may also directly ~~also directly~~ lead to *final failure* (as for example in the case of Puck's torsion spring [7]) of a laminate via the development of through-thickness stresses and~~or, via~~ a following local delamination, and hence to~~hence, to~~ 'wedge buckling' of an adjacent lamina~~and therefore to final failure of the laminate~~. So, the IFF3 mode, where parts of a lamina move in the thickness direction, may initiate a catastrophic FF, **Fig. 4.** The grade of criticality is depicted in **Fig. 5**. It depends on the lay-up: A *tension*-loaded outer hoop layer of a pressure vessel experiences highest criticality, too.

In the context above a further aspect is to be mentioned: The difference between isolated and embedded lamina behaviour comes from the effect of the occurrence of single micro-cracks in the isolated case. The critical one of them grows to macro-size and causes fracture, whereas in the embedded case multi-site micro-cracking is generated. The latter is induced by the strain-control of the neighbouring layers. Figure 4 also informs about the specific IFF features of isolated and embedded laminae.

3 The Failure Mode Concept (FMC)

The FMC generates a phenomenological three-dimensional lamina stress-based engineering approach for the derivation of failure conditions. **Table 1** summarizes the main features of the FMC. The FMC regards mechanics and probabilistics in the interaction zones of the failure modes, thus finally leading back to a formulation that looks like a so-called 'single or global failure surface'.

Table 2 depicts the system of strength failure domains from 'onset of yielding' (if applicable) to 'onset of fracture'. In addition, the table points out the 5 failure modes: $F_{\|}^{\sigma} \rightarrow$ FF1, $F_{\|}^{\tau} \rightarrow$ FF2, $F_{\perp}^{\sigma} \rightarrow$ IFF1, $F_{\perp\|} \rightarrow$ IFF2, $F_{\perp}^{\tau} \rightarrow$ IFF3. These failure modes shall be reported now in its 3D formulations but with a newly formulated IFF2. Later, the 2D IFF2 formulation will be derived.

3.1 FMC-based 3D-fracture Failure Conditions

Applying FMC methodology to UD material is to~~strictly~~ propose a set of equations describing ~~for a number of~~five failure modes in each~~the~~individual lamina (ply) and then to combine these equations in a suitable manner to predict failure in a lamina in order to consider the superposition of *all* modes, see Ref[1]).

Each failure mode is described by a distinct failure function *F*

~~Part B , set~~ $FF1: \quad F_{\|}^{\sigma} = \dfrac{I_1}{\bar{R}_{\|}^{t}} \quad , \qquad FF2: \quad F_{\|}^{\tau} = \dfrac{-I_1}{\bar{R}_{\|}^{c}} \quad ,$

$IFF\,1: \quad F_{\perp}^{\sigma} = \dfrac{I_2 + \sqrt{I_4}}{2\bar{R}_{\perp}^{t}} \quad , \qquad IFF\,3: \quad F_{\perp}^{\tau} = (b_{\perp}^{\tau} - 1)\dfrac{I_2}{\bar{R}_{\perp}^{c}} + \dfrac{b_{\perp}^{\tau}\sqrt{I_4}}{\bar{R}_{\perp}^{c}} \quad ,$ (1a-1e)

$IFF\,2: \quad F_{\perp\|} = \dfrac{I_3^{3/2}}{\bar{R}_{\perp\|}^{3}} + b_{\perp\|}\dfrac{I_2 I_3 - I_5}{\bar{R}_{\perp\|}^{3}} = \left(\dfrac{\tau_{31}^{2} + \tau_{21}^{2}}{\bar{R}_{\perp\|}^{3}}\right)^{3/2} + b_{\perp\|}\dfrac{\sigma_2 \cdot \tau_{21}^{2} + \sigma_3 \cdot \tau_{31}^{2}}{\bar{R}_{\perp\|}^{3}}$

containing terms~~which~~ that imply an ***interaction between***~~the~~ the various active ***~~acting~~ stresses*** *(stress tensor components)*~~es~~. The invariants utilized are

$$I_1 = \sigma_1 \,, \qquad I_2 = \sigma_2 + \sigma_3 \,, \quad I_4 = (\sigma_2 - \sigma_3)^2 + 4\tau_{23}^2 \qquad \text{(1f-1j)}$$

$$I_3 = \tau_{31}^2 + \tau_{21}^2, \quad I_5 = (\sigma_2 - \sigma_3)(\tau_{31}^2 - \tau_{21}^2) - 4\tau_{23}\tau_{31}\tau_{21}\,.$$

They were derived by Boehler [11]. I_5 considers the physical difference of $\tau_{21}(\sigma_2)$ to $\tau_{31}(\sigma_2)$.

If the stresses, inserted into the failure functions *F*, are fracture stresses this leads to ***fracture conditions*** when setting *F=100%* or mode-wise $F^{mode}(\sigma_i,\ \bar{R}^{mode}) = 1$, *respectively*. The FE output stresses are to be inserted as input values in these equations when computing the reserve factors.

Remind: The 2nd term in I_5 $(4\tau_{23}\tau_{31}\tau_{21})$ was deleted because on one side this combination is very seldom of importance, and on the other side can be made zero if a transformation in the quasi-isotropic plane is accomplished via $(\sigma_1,\sigma_2,\sigma_3,\tau_{23},\tau_{31},\tau_{21}) \rightarrow (\sigma_1,\sigma_2^{*},\sigma_3^{*},0,\tau_{31}^{*},\tau_{21}^{*})$.

In the equations above, $\bar{R}$ denotes a *mean* or *typical* strength value that is to be used in *stress/ deformation analysis*. Later a letter *R* will be applied. It is either a general value or the so-called *design allowable* which is a statistically-based minimum value to be used in *strength analysis*.

Besides the *design-mandatory* 5 strengths the Eqs(1) ~~hasve been derived with~~ contain two ~~free~~ *curve parameters* $(b_{\perp\|},\ b_{\perp}^{\tau})$ that are ~~to be~~to be determined from multi-axial test data in the associated 'pure domain of validity' of the respected mode or can be estimated by experience. ~~$\overline{R}$ marks mean strength value~~ Simplified, one ~~fibre~~ calibration point □ for each of the two modes delivers, after inserting its coordinates into the IFF conditions: for $F_{\perp\|}$ from a point $\left(\sigma_2^{\ c},\ \tau_{21}^{\perp\|}\right)$ (see [1, 2]) and for $F_{\perp}^{\tau}$ from $(\sigma_2^{c\tau},\sigma_3^{c\tau})$, and after a resolving the two equations (2)

$$b_{\perp\|}=\frac{1-\left(\tau_{21}^{\perp\|}/\overline{R}_{\perp\|}\right)^2}{2\sigma_2^{c}\cdot\tau_{21}^{\perp\|2}/\overline{R}_{\perp\|}^{3}} \qquad \text{and } \textit{Part B set} \quad b_{\perp}^{\tau}=\frac{1+(\sigma_2^{c\tau}+\sigma_3^{c\tau})/\overline{R}_{\perp}^{c}}{(\sigma_2^{c\tau}+\sigma_3^{c\tau})/\overline{R}_{\perp}^{c}+\sqrt{(\sigma_2^{c\tau}-\sigma_3^{c\tau})^2}/\overline{R}_{\perp}^{c}}\,.$$

(2a, 2b)

The author's experience with test data leads to the conclusion: Safe b~~B~~ounds~~on the safe side~~ for typical epoxy containing GFRP, CFRP and AFRP are~~were assumed to be~~ $0.05<b_{\perp\|}<0.2$ *and* $1.0<b_{\perp}^{\tau}<1.1$. A value $b_{\perp\|}=0$ means there is 'no bulge effect' or increase of shear resistance in compression domain, see **Fig.6**. A value $b_{\perp}^{\tau}=1$ means 'no material friction' is existing in the quasi-isotropic ⊥⊥-plane (not active in 2D case, see [Cun03]). As calibration points for $b_{\perp}^{\tau}$ are still missing (brittle isotropic materials however give some good information),~~: A~~ $b_{\perp}^{\tau}=1$ during ~~a~~pre-dimensioning~~.~~ is recommended as it provides a safe lower bound.~~to behaviour of many unidirectional laminae will keep the engineer in the compression domain on the safe side. It furthermore will simplify the failure function~~ By setting $b_{\perp\|}=b_{\perp}^{\tau}=0$ the FMC-based equations are simplified 'down' to the level of the Tsai/Wu model [12]~~a good approach~~.

The FF1 cannot be described by a homogenized (smeared) macroscopical stress value σ_1. So, the engineering-like macroscopical modelling has to be replaced by a correct microscopical one, however, shall be 'approximately' formulated in macroscopical quantities. This is the FEA-computed macro-mechanical strain ε_1. *Remind* from [2] *IFF1*: $F_{\|}^{\sigma}$: $I_1=\sigma_1 \approx \nu_f\cdot\sigma_{1f}=\nu_f\cdot\varepsilon_1\cdot E_{1f}=\varepsilon_1\cdot E_{\|}$ with σ_{1f} = tensile fibre stress which is responsible for fracture. No fibre properties are required.

With regard ~~respect~~ to the 3D nature ~~character~~of the *lamina* IFF conditions, ~~-~~both, ~~above~~IFF1 ($F_{\perp}^{\sigma}$:= transverse tensile failure, cracking due to inter-laminar stresses $\sigma_3^{t},\tau_{32},\tau_{31}$) and IFF3 ($F_{\perp}^{\tau}$:= wedge failure, the intra-laminar stresses σ_2^{c},τ_{21} may cause cracking and a local 3D stress state including σ_3) also serve ~~($F_{\perp}^{\tau}$: wedge failure, $F_{\perp}^{\sigma}$: transversal tensile failure)~~ as criteria for the 'onset of delami-nation' which is a *laminate* failure type.

Note: F = 1 is termed failure condition. It mathematically describes the limit state or fracture surface. F >=< 1 is termed failure criterion.

3.2 Mode Reserve Factors

Determination of Mode Reserve Factors

Employing the mode's *strength* $\overline{R}^{mode}$ and its *equivalent stress* σ_{eq}^{mode} for linear analyses, according to the general equation $f_{Res}^{(mode)} = \overline{R}^{mode} / \sigma_{eq}^{mode}$, the following set of formulae for the *reserve factor* of each mode can be provided [2]

FF 1 $$f^{||\sigma} = \overline{R}_{||}^{t} \; / \; (\varepsilon_1 \cdot E_{||}) \; = \; R_{||}^{t} \; / \sigma_{eq}^{||\sigma} \,, \qquad (3a)$$

FF 2 $$f^{||\tau} = -\overline{R}_{||}^{c} \; / \; \sigma_1 \quad = +\overline{R}_{||}^{c} \; / \; \sigma_{eq}^{||\tau} \,,$$ ~~Part B set~~

(3b)

IFF 1 $$f^{\perp\sigma} = 2\overline{R}_{\perp}^{t} \; / \; [(\sigma_2+\sigma_3) \; + \; \sqrt{\sigma_2{}^2 - 2\sigma_2\sigma_3 + \sigma_3{}^2}\,] \; = \overline{R}_{\perp}^{t} \; / \sigma_{eq}^{\perp\sigma} \,, \qquad (3c)$$

IFF 2 $$f^{\perp||} = \overline{R}_{\perp||} \; / \; [(\tau_{31}{}^2 + \tau_{21}{}^2)^{3/2} + \; 2b_{\perp||}(\sigma_2 \cdot \tau_{21}{}^2 + \sigma_3 \cdot \tau_{21}{}^2)]^{1/3} = \overline{R}_{\perp||} / \sigma_{eq}^{\perp||} \,, \qquad (3d)$$

IFF 3 $$f^{\perp\tau} = -\overline{R}_{\perp}^{c} \; / \; [(b_{\perp}^{\tau} - 1) \cdot (\sigma_2+\sigma_3) + b_{\perp}^{\tau} \sqrt{\sigma_2^{\,2} - 2\sigma_2\sigma_3 + \sigma_3^{\,2}}\,] \; = +\overline{R}_{\perp}^{c} \; / \sigma_{eq}^{\perp\tau} \,. \qquad (3e)$$

In case of e.g. tensile stresses, due to an automatic insertion taken later for reasons of having one single equation instead of dealing with several equations, the reserve factors for FF2 and IFF3 will become negative. This means there is no stressing of the material. In a later section will be reported how this problem is numerically treated.

An equivalent stress σ_{eq} (always positive such like the strengths) includes all actual load stresses and residual stresses that are acting together in a given mode ~~equation~~.

Simplification of the 3D IFF2 formulation

In the WWFE, the single numerical problem (probably no intersection is achieved of mode curve IFF3 with curve IFF2, **Fig. 7**) of the 3D conditions was bypassed by a query, that requires $\tau_{21} \leq max\tau_{21}$. The determination of the bound value $max\,\tau_{21}$ is performed in Appendix B of Ref [2] This problem can be tackled when leaving the usual *principle of proportional stressing* (all stresses of the actually given stress state are equally factored), which interprets the mode reserve factors as mode stretch factors of the actual stress vector. Stretching ends when the associated mode failure curve is met. Figure 7 visualises this procedure.

A violation of this principle should be permitted if 'mapping of the interaction of failure modes' is addressed. Now, instead of factoring the full stress state in Eq.3e that means factoring each stress,

just the mode driving shear stresses and not the transversal normal stresses are factored. Unfortunately this equation includes factors wit power 4 and 3, which has no solution. Therefore, the approach is modified to having factors with the powers 4 and 2

$$\overline{R}_{\perp\|}{}^4 = f^{\perp\|4}\cdot(\tau_{31}{}^2+\tau_{21}{}^2)^2 + f^{\perp\|2}\cdot 2bb_{\perp\|}\cdot(\sigma_2\cdot\tau_{21}{}^2+\sigma_3\cdot\tau_{31}{}^2)\cdot\overline{R}_{\perp\|}\,. \qquad (4)$$

The root of Eq. (4) delivers for the 3D stress state (a negative root makes no sense)

$$f^{\perp\|} = \sqrt{-ba+\sqrt{ba^2+1/a}}\,, \qquad (5)$$

with $ba = b/2a\,,\quad b = 2bb_{\perp\|}\cdot(\sigma_2\cdot\tau_{21}{}^2+\sigma_3\cdot\tau_{31}{}^2)/\overline{R}_{\perp\|}{}^3\cdot\,,\quad a = \cdot(\tau_{31}{}^2+\tau_{21}{}^2)^2/\overline{R}_{\perp\|}{}^4\,,$ (6a)

and for the 2D stress state ($bb_{\perp\|} \neq b_{\perp\|}$)

$$ba = b/2a\,,\quad b = 2bb_{\perp\|}\cdot(\sigma_2\cdot\tau_{21}{}^2)/\overline{R}_{\perp\|}{}^3\cdot\,,\quad a = \tau_{21}{}^4/\overline{R}_{\perp\|}{}^4\,. \qquad (6b)$$

This procedure takes the former non-intersection problem completely away. Probable slight differences in mapping, when applying this numerically advantageous simplification may be balanced by the 'choice' of the parameter $bb_{\perp\|}$ and a little by $\dot{m}$. Mapping is executed equally well.

3.4 Interaction of Failure Modes or Determination of Resultant Reserve Factors

Mechanical and probabilistic interactions cannot be clearly distinguished and therefore, Cuntze models the failure mode interactions by a simple probabilistically based 'series spring model' approach [1, 2 ~~for describing the combined effect of this system of failures~~]. Such a model describes the lamina failure system as a series failure system. A series system is in a state of failure whenever any of its elements fails. Each mode is one element of the failure system and is seen to be independent of the other.

By this method, the *interaction between* FF and IFF *modes* as well as between the various IFF modes acts as a rounding-off procedure linked to the determination of the desired values for the most often permitted (if linear analysis is sufficient) stress-based resultant reserve factor f_{Res}. In these mixed failure domains the desired f_{Res} ~~(super-script res)~~automatically takes into ~~the~~ account ~~of~~ the interactions between all the affected ~~of all~~ modes in utilizing the formula

$$(1/f_{Res})^{\dot{m}} = \Sigma\,(f_{Res}^{modes})^{\dot{m}} \text{ ..... for linear analysis} \qquad (7a)$$

$$= (1/f_{Res}^{\perp\sigma})^{\dot{m}} + (1/f_{Res}^{\perp\|})^{\dot{m}} + (1/f_{Res}^{\perp\tau})^{\dot{m}} + (1/f_{Res}^{\|\sigma})^{\dot{m}} + (1/f_{Res}^{\|\tau})^{\dot{m}}\,,$$

or fully equivalent in case of linear analysis, then $1/f_{Res} = Eff$,

$$(Eff)^{\dot{m}} = \Sigma(Eff^{modes})^{\dot{m}} \text{ ..... for linear and non-linear analysis} \qquad (7b)$$

$$= (Eff^{||\sigma})^{\dot{m}} + (Eff^{||\tau})^{\dot{m}} + (Eff^{\perp\sigma})^{\dot{m}} + (Eff^{\perp||})^{\dot{m}} + (Eff^{\perp\tau})^{\dot{m}},$$

~~as the **resultant Effort** (interaction of failure modes),~~ in which ~~ith~~ $\dot{m}$ is~~as~~ the mode interaction coefficient. It is also termed rounding-off exponent, the size of which is high in case of low scatter and vice versa. As a simplifying ~~practical simplifying~~ *assumption,* $\dot{m}$ is given here the ~~taken~~same value, regardless of mode ~~for each~~interaction zone! The value of $\dot{m}$ is obtained by curve fitting~~has to be set by fitting~~~~This experience is gained from that -and by respecting the fact -still given above- that~~. The author's experience suggests that ~~, but~~ $\dot{m} = 3.1$ is often appropriate, the more, if a lamina is embedded in a laminate~~gives a good approximation~~~~is a good approach~~.

In practice, at maximum 3 modes of the possible 5 ones will physically interact. However, all modes are included in Eqs.(7) in order to always have the full set of equations in one equation during the numerical analysis. If an $f_{\mathrm{Re}\,s}^{(\mathrm{mod}\,e)}$ becomes negative, caused by the numerically advantageous, sign-considering automatic insertion of the FEA stress output $\{\sigma\}=(\sigma_1,\sigma_2,\sigma_3,\tau_{23},\tau_{13},\tau_{12})^T$ into *all* 5 failure conditions, a value of *100* shall replace a negative $f_{\mathrm{Re}\,s}^{(\mathrm{mod}\,e)}$, and a zero shall replace its equivalent stress value. A query serves to exclude such a negative or zero value. For the specific 2D failure conditions in the section 4 the queries can be avoided by the application of absolute values in the associated failure equation, see FF1 and FF2 in the MATHCAD program attached as Annex. Of course, one can also take the full set of possible mode combinations and choose the applicable ones after sorting out those which do not make sense.

If ~~eg inserting~~ a unidirectional fracture stress (i.e.~~this is~~ the strength value $\overline{R}_{\perp}^{t}$) is inserted into the equation above, then a point on a 2D-failure curve or on the3D-failure surface, described by $F = 1$ or $f_{Res} = 1$ or $EFF = 1$, is achieved~~, the strength point~~. A failure surface is the result of an optimally mapping of the course of test data and, therefore, is characterized by a 50% survival probability.

Rounding-off, by employing Eq(7), in mode interaction zones of adjacent *mode failure curves* (2D) and *partial* failure surfaces (3D) is leading again to a *global* failure curve and surface, or –in other words-, to a 'single surface failure description' such as with Tsai/Wu [12], however, without the well-known shortcomings.

4 *2D*-Failure Conditions with Determination of Failure Curves

4.1 Derivation of the 2D $F_{\perp||}$ approach

Focussing a 2D state of stress $\{\sigma\}=(\sigma_1,\sigma_2,0,0,0,\tau_{21})^T$ the failure conditions become simpler than those dedicated to the 3D case, but, all failure conditions and strengths remain active: The 3D IFF2 condition of the WWFE (Eq.1d), reduced to 2D, leads to the associated mode reserve factor

$$f^{\perp\|} = \bar{R}_{\perp\|} / \left[\tau_{21}{}^3 + 2b_{\perp\|}\sigma_2 \cdot \tau_{21}{}^2\right]^{1/3}. \tag{8}$$

Of course, even for this simpler formulation the problem needing a query in the code [2] still exists. Therefore, in the 2D case approach Cuntze circumvents this shortcoming by replacing the invariant-based formulation by the simplest formulation possible, the linear formulation [13]

$$F_{\perp\|} = \frac{|\tau_{21}|}{(\bar{R}_{\perp\|} - B_{\perp\|}\cdot\sigma_2)} \ . \tag{9a}$$

This approach fully corresponds to the Mohr–Coulomb formulation $\tau_n = R_\tau - \mu\sigma_n$ with Mohr's fracture stresses τ_n, σ_n acting on the section plane and μ the UD Material's internal friction coefficient, see Ref.[14].

From this, applying the principle of proportional stressing for all stresses applied follows

$$\frac{f_{\perp\|}\cdot|\tau_{21}|}{(\bar{R}_{\perp\|} - B_{\perp\|}\cdot f_{\perp\|}\cdot\sigma_2)} = 1 \tag{10a}$$

or resolved for the mode reserve factor

$$f^{\perp\|} = \bar{R}_{\perp\|} / \left[|\tau_{21}| + B_{\perp\|}\sigma_2\right] . \tag{10b}$$

But this formulation contains a drawback because this τ_{21}-driven condition in contrast to Eq.8 still exists if $\tau_{21} = 0$ and $\sigma_2 \neq 0$. This problem is bypassed in the same way as in the case the 3D IFF2 condition, by factoring in Eq.9 just the driving stress τ_{21}, thus yielding ($B_{\perp\|} \neq 2bb_{\perp\|}$ or $2b_{\perp\|}$)

$$f^{\perp\|} = (\bar{R}_{\perp\|} - B_{\perp\|}\cdot\sigma_2)/\tau_{21} \tag{11a}$$

or the stress effort which is to be utilized in non-linear analysis

$$Eff^{\perp\|} = \tau_{21}/(\bar{R}_{\perp\|} - B_{\perp\|}\cdot\sigma_2) . \tag{11b}$$

Just one curve parameter, the internal friction characterizing parameter $B_{\perp\|}$, has to be determined in the 2D case.

4.2 Yield condition and Fracture Conditions

Yield Condition

According to the FMC for the transversally-isotropic material, similarly to isotropic materials, just terms describing the shape change of the UD material cube can contribute to a failure function. Based on this, for the failure mechanism yielding, the proposed approach yields the ***yield condition***

$$F_y = \frac{\sigma_2}{(\overline{R}_{\perp\|p0.2})^2} + \frac{{\tau_{21}}^2}{(\overline{R}^c_{\perp p0.2})^2} = {a_y}^2 \qquad (12)$$

(preliminary formulation in WWFW [2]) with the size parameter a_y and the two yield strengths $\overline{R}_{\perp\|p0.2}, \overline{R}^c_{\perp p0.2}$, at a permanent plastic strain of 0.2% dedicated to the two non-linear stress-strain curves $\tau_{21}(\gamma_{21})$ and $\sigma^c_2(\varepsilon_2)$. Its regime is growing from the yield initiation value 1 due to $1 \le a_y \le$ *IFF value*. The yield failure curve is of importance e.g. for indicating damage begin and for creeping in case of not well-designed laminates.

Above condition involves two yield strength values what seems to be in contradiction to the FMC. But, these values are highly correlated due to the matrix material the yield strength value of which is the governing quantity. Figure 20 in Ref. [2] visualizes how the ($\tau_{21}(\sigma_2)$ initiation yield or onset of yielding curve lies within the IFF envelope. This so-called single (global) *yield* surface is confined by the five partial fracture surfaces formulated below.

Fracture Conditions

After substitution of the former $F_{\perp\|}$ the full set of 2D failure conditions reads

$$\text{~~Part B , set~~}\ FF1\ldots\ F^{\sigma}_{\|}: \ \frac{\varepsilon_1 \cdot E_{\|}}{\overline{R}^t_{\|}} = 1, \quad FF2\ldots\ F^{\tau}_{\|}: \ \frac{-\sigma_1}{\overline{R}^c_{\|}} = 1,$$

$$IFF\ 1\ldots\ F^{\sigma}_{\perp}: \ \frac{\sigma_2}{\overline{R}^t_{\perp}} = 1, \quad IFF\ 2\ldots\ F_{\perp\|}: \ \frac{|\tau_{21}|}{\overline{R}_{\perp\|} + B_{\perp\|} \cdot \sigma} = 1, \qquad (13a\text{-}e)$$

$$IFF\ 3\ldots F^{\tau}_{\perp} = \frac{-\sigma_2}{\overline{R}^c_{\perp}} = 1,$$

with stresses being fracture stresses. The remaining curve parameter $B_{\perp\|}$ is determined by curve fit simulation. Its value is, due to the linear formulation, much higher than the value of $b_{\perp\|}$, [2]. In section 4.5 distinct $B_{\perp\|}$ values are given for the test data curves which have been mapped by the Eqs(13).

4.3 Establishment of 2D Failure Surfaces and Failure Curves

Under the assumption “No residual stresses are acting” the associated three interesting failure surfaces are presented:

IFF Envelope or Fracture Curve $\tau_{21}(\sigma_2)$

According to the Eqs(7, 11a), the formulation of the IFF fracture envelope -zero fibre stress- reads

$$(1/f_{Res}^{IFF})^{m} = \left(\frac{\sigma_2}{\overline{R}_{\perp}^{t}}\right)^{m} + \left(\frac{|\tau_{21}|}{\overline{R}_{\perp||} \cdot -B_{\perp||} \cdot \sigma_2)}\right)^{m} + \left(\frac{-\sigma_2}{\overline{R}_{\perp}^{c}}\right)^{m} = 1. \qquad (14a)$$

The afore-mentioned smart formulation of Mr. Freund, utilized in the attached code, avoids the queries. It reads

$$(1/f_{Res}^{IFF})^{m} = \left(\frac{\sigma_2 + |\sigma_2|}{2\overline{R}_{\perp}^{t}}\right)^{m} + \left(\frac{|\tau_{21}|}{\overline{R}_{\perp||} \cdot -B_{\perp||} \cdot \sigma_2)}\right)^{m} + \left(\frac{-\sigma_2 + |\sigma_2|}{2\overline{R}_{\perp}^{c}}\right)^{m} = 1. \qquad (14b)$$

The conditions in the 3D case, Eqs(3), are formally the same.

IFF Failure Surface or Failure Body $(\sigma_1, \sigma_2, \tau_{21})$

For bi-axial stress states $\{\sigma\}=(\sigma_1, \sigma_2, 0, 0, 0, \tau_{21})^T$ the formulation of the global IFF fracture envelope, including FF-IFF interaction, reads

$$(1/f_{Res})^{m} = \qquad (15a)$$

$$= \left(\frac{(\varepsilon_1 + |\varepsilon_1|) \cdot E_{||}}{2\overline{R}_{||}^{t}}\right)^{m} + \left(\frac{-\sigma_1 + |\sigma_1|}{2\overline{R}_{||}^{c}}\right)^{m} + \left(\frac{\sigma_2 + |\sigma_2|}{2\overline{R}_{\perp}^{t}}\right)^{m} + \left(\frac{|\tau_{21}|}{\overline{R}_{\perp||} - B_{\perp||} \cdot \sigma_2}\right)^{m} + \left(\frac{-\sigma_2 + |\sigma_2|}{2\overline{R}_{\perp}^{c}}\right)^{m} = 1$$

With Eq(15a) the complete failure surface or body can be computed. It is visualized in **Fig.8**. Of course, *Eq(15a)* can deal with stresses from a non-linear analysis which considers the non-linear strain-hardening.

FF Failure Surface = Final Failure

The formulation of the final failure curve takes into account. hardening, softening and geometrical non-linearity. It reads

$$(1/f_{Res}^{final})^{m} = \left(\frac{(\varepsilon_1 + |\varepsilon_1|) \cdot E_{||}}{2\overline{R}_{||}^{t}}\right)^{m} + \left(\frac{-\sigma_1 + |\sigma_1|}{2\overline{R}_{||}^{c}}\right)^{m} + \left(\frac{-\sigma_2 + |\sigma_2|}{2\overline{R}_{\perp}^{c}}\right)^{m} = 1. \qquad (15b)$$

Figure 7 further depicted the domains where FF and IFF are practically not interacting. In these domains IFF and FF can be treated decoupled and the separate utilization of an IFF condition is permitted. In the FF domains fibre stresses govern whereas in the IFF domains the stresses σ_2 and τ_{21} dominate.

4.4 Verification of Conditions by Lamina and Laminate Test Cases

Main cross-section of the 2D stress state's failure body is the plane $(\tau_{21}(\sigma_2)$. The **Figures 9** and **10** outline the *mapping* capabilities of the 3D and the 2D conditions. In this specific test case, provided by WWFE the course of test data is also mapped with a very good result. (*Mind*: the author assumes the very high τ_{21} value on the bulge, point ?, is not correctly measured or evaluated, respectively). All material parameters utilized for mapping are included in the captures as well as the different curve parameters for reasons to compare with the 2D-reduced 3D conditions. For the 2D and 3D formulations equal parameters practically deliver identical curves. The two remaining sections or failure envelopes are the planes $\tau_{21}(\sigma_1)$ and $\sigma_2(\sigma_1)$ are not affected by the change in IFF2. Visualisations are found in WWFE [1, 2].

A confirmation of the 2D conditions by laminate test cases shall not be performed in the frame of the paper at hand. However, as the 2D conditions map 2D test cases the same as the 3D conditions Eq(3) do, one can transfer the conclusion from WWFE: The correlation between the author's predictions and the experimental data (just 2D data was delivered) are generally satisfactory for the laminates, especially where Fibre Failure (FF) is the dominant mode, which is the case for -due to netting theory- well-designed laminates.

5 Determination of Reserve Factor and Margin of Safety

5.1 Design Aspects

According to the normally applied safety concept 'Loads are increased by a factor of safety' (denoted FOS j) the reserve factors, which have to be determined for the *Design Verification* of the laminate, are also *load*-related defined. To achieve the verification of the design the designer must know: Is the actual load case, which might involve several strength and other failure modes, failure critical or not? Generally, there are two failure load limit states to be regarded, the ***initial failure load*** and the ***final failure load***. For instance, leak failure belongs to another failure mode and cannot be predicted by the Eq(14. Initial failure more or less corresponds to IFF and final failure to fibre failure regarding 'wedge failure'.

Initial failure stresses are important where a standard requires a Design Verification with respect to IFF. This means: At Design Limit Load level (*DLL*) no IFF is permitted. Such applications may be fatiguing of structures, or rotors which require a low out-of-balance.

For the Design Verification at the higher ultimate load level ($DUL=j_{ult}\cdot DLL$) the accuracy of the initial failure prediction as an intermediate step has not that much impact because IFF influence reduces with increasing degradation. Beyond IFF, often termed *post failure* regime, the failure body is laterally shrinking and the non-linear behaviour leads to a load-redistribution, which means to a

reduction of IFF stresses on cost of higher fibre stresses. This is correlated with vanishing residual stresses. The points 1 and 2 in **Fig. 11** highlight the degradation-dependent laterally shrinking of the '2D failure body' when coming beyond the IFF level.

As the two design verification types *initial* and *final failure* shall not occur a minimum reserve factor ≥ 1 is required. This is performed in respecting the formulae:

- for the *initial failure*, indicated by the so-called knee in the laminate's stress-strain curve and

originated by $F_{\perp}^{\sigma}$, $F_{\perp\parallel}$, $(F_{\perp}^{\tau})$ $\qquad f_{\mathrm{Re}s}^{initial} = \dfrac{initial\ \ failure\ \ load}{j_{init} \cdot DLL}$, (16a)

- for the *final failure*, indicated by $F_{\parallel}^{\sigma}$, $F_{\parallel}^{\tau}$ and $F_{\perp}^{\tau}$ $\qquad f_{\mathrm{Re}s}^{final} = \dfrac{final\ \ failure\ \ load}{j_{ult} \cdot DLL}$ (16b)

with j_{init} , j_{ult} : = design factors of safety. It is assumed $j_{init} \approx j_{p0.2}$. Values for the FoS are, e.g. in aerospace, $j_{p0.2=1.1}$ and $j_{ult} = 1.25$. Due to the redundancy in a laminate it is recommended to set $j_{initial} = 1.0$.

Design factors of safety for spacecrafts are found in the ECSS Standards of ESA/ESTEC, e.g. for high pressurized structures and vessels in [15].

If laminates are well-designed (netting theory applied, fibre-dominated) straining up to *final* failure is pretty linear. Due to this fact, stresses and loads are relatively linearly related. Not well-designed laminates always require a high non-linear effort to compute accurate stresses, strains, and deformations.

S*trength design allowables* (**Fig. 12**) are smaller than the mean strengths also termed typical strengths, $R_i < \overline{R}_i$. Therefore, the effective stress-strain non-linearity - when computing the initial failure load- is not so high, see subsection 5.3. Further workload-reducing, that means the application of linear analysis is good enough, act the FoS j which are applied when designing. The higher the FOS, the more the assumption of a simple linear structural analysis is justified to compute the stresses and strains in the critical lamina.

Of further importance is the very commonly applied '*design strain* of $\varepsilon \approx 0.35\%$', required as a damage tolerance considering value at Design Limit Load level. Applying this design strain, linear analysis is practically sufficient. This value also covers the design case initial failure.

When performing design work one should keep in mind for the sake of simplifying the analysis as far as possible: Design a laminate to be stable as a truss (netting theory applicable) and stack the laminae at angles to generate a laminate robust against possible load changes. This will lead to a well-designed laminate and to the freedom to model the laminate behaviour by linear analysis.

In the following sub-sections, the way is presented how mode reserve factors f_{Res}^{mode} and global reserve factor f_{Res} have to be determined. It is demonstrated for the 2D conditions, only.

5.2 Stress-based Reserve Factor *(linear structural analysis acceptable, $\{\sigma\}_L = j\cdot\{\sigma(DLL)\}$)*

The reserve factor f_{Res} is defined here that factor all *mechanical load*-induced stresses applied have to be multiplied with to generate failure. Geometrically it means that the stress vector $\{\sigma\}_L$ has to be stretched in its direction by this factor till the failure surface, Figure 7. This procedure is called 'principle of proportional stressing' and is valid as far as *linear* modelling can be applied. If high design *factors of safety* (FoS) are required and if there are no residual stresses, then linear elastic modelling is almost always permissible and just a stress-based f_{Res} needs to be predicted.

Initial (IFF) Proof of Design: *Initial* failure load ≥ Design *Limit* Load (j =1)

- Case "No residual stresses", Figure 12: $\{\sigma\}_L$ contains mechanical load stresses, only

In general case of a *global* failure condition –such as with Tsai/Wu- the insertion of

$$\{\sigma\}_{failure} = f_{Res}\cdot\{\sigma\}_L \quad \equiv \quad \{\sigma\}_L + MS\cdot\{\sigma\}_L \qquad \textit{proportional stressing} \tag{17}$$

into the failure conditions will deliver a polynomial equation for f_{Res} the explicit solubility of which might be possible or not. Applying the FMC, the solution procedure becomes simpler because just *mode* reserve factors have to be determined and the desired resultant (or global) reserve factor as a function of the mode reserve factors is computable.

Inserting $$\{\sigma\}_{failure}^{mode} = f_{\mathrm{Res}}^{mode}\cdot\{\sigma\}_L \tag{18a}$$

into the Eqs(13) or, in other words, multiplying each stress in the Eqs(13) by the associated f_{Res}^{mode}, each 2D f_{Res}^{mode} can be extracted

$$f^{||\sigma} = \bar{R}_{||}^{t}/(\varepsilon_1\cdot + |\varepsilon_1|)E_{||}), \quad f^{||\tau} = -2\bar{R}_{||}^{c}/(\sigma_1 - |\sigma_1|), \text{ ~~Part B set~~}$$

(19a-e)

$$f^{\perp\sigma} = 2\bar{R}_{\perp}^{t}/(\sigma_2 + |\sigma_2|), \quad f^{\perp||} = (\bar{R}_{\perp||} - B_{\perp||}\cdot\sigma_2)/|\tau_{21}|, \quad f^{\perp\tau} = -2\bar{R}_{\perp}^{c}/(\sigma_2 - |\sigma_2|),$$

The minimum value outlines which mode reserve factor is the design driving one.

Afterward, in order to compute f_{Res}^{IFF}, the mode reserve factors are inserted into the Eqs(20)

$$(1/f_{Res}^{IFF})^m = (j/f^{||\sigma})^m + (j/f^{||\tau})^m + (j/f^{\perp\sigma})^m + (j/f^{\perp||})^m + (j/f^{\perp\tau})^m. \tag{20}$$

- Case "With residual stresses", **Fig. 13**

Inserting into the Eqs(13) $\{\sigma\}^{mode}_{failure} = f^{mode}_{Res} \cdot \{\sigma\}_L + \{\sigma\}_R$, (18b)

with the *residual stress vector* $\{\sigma\}_R$ from curing, yields an equation for each *stress-based* f^{mode}_{Res}

$f^{||\sigma} = (\bar{R}^t_{||} - \sigma_{1R})/(\varepsilon_1 \cdot E_{||})$, $f^{||\tau} = -(\bar{R}^c_{||} - \sigma_{1R})/\sigma_1$, ~~Part B set~~

(21a-e)

$f^{\perp\sigma} = (\bar{R}^t_{\perp} - \sigma_{2R})/\sigma_2$, $f^{\perp||} = (\bar{R}_{\perp||} - \tau_{21R} - B_{\perp||} \cdot \sigma_2)/\tau_{21}$, $f^{\perp\tau} = -(\bar{R}^c_{\perp} - \sigma_{2R})/\sigma_2$

Once more, these equations have to be inserted into the Eqs(20). This procedure is permitted as long as the stresses have not caused an essential amount of damage that would lead to stress-redistribution and to a reduction of the size of the residual stresses. For the sake of a simple formulation the 'smart type' has not been chosen.

Final (FF) Proof of Design: *Final* failure load' > Design *Ultimate* Load ($j=j_{ult}$)

The determination of the *final failure load*, necessary for the *Ultimate Design Verification*, utilizes the

Eqs(15). Because probable remaining marginal residual stresses at failure have no load-carrying effect anymore there is just the case 'No residual stresses' to be treated. The remaining mode reserve factors read

$$f^{||\sigma} = 2\bar{R}^t_{||}/((\varepsilon_1 + |\varepsilon_1|) \cdot E_{||}) = R^t_{||}/\sigma^{||\sigma}_{eq},\ f^{||\tau} = -2\bar{R}^c_{||}/(\sigma_1 - |\sigma_1|) = -\bar{R}^c_{||}/\sigma^{||\tau}_{eq} \quad (21)$$

However, if wedge failure is essential Eq.20 has to be replaced with Eq.22

$$(1/f^{final}_{Res})^m = (j/f^{||\sigma})^m + (j/f^{||\tau})^m + (j/f^{\perp\tau})^m \quad (22)$$

5.3 Load-based Reserve Factor *(non-linear structural analysis applied , $\{\sigma\}_L = \{\sigma(j \cdot DLL)\}$)*

Beyond IFF the essential features in the associated non-linear analysis are:

* Loading is re-distributed versus fibres,
* Load path is altering in contrast to the linear case, and
* Large strains and deformations may occur.

A*ccurate* reserve factors have to be referred to loads, which means, according to their original definition. Instead of the stress formulation

$$f_{Res} = \frac{design\ allowable\ "strength"}{j \cdot \sigma(DLL)} = \frac{R}{j \cdot \sigma(DLL)} \quad (23a)$$

of the linear case (strength *R*= stress resistance), in the non-linear case, the load formulation

$$f_{Res} = \frac{design\ allowable\ "load\ resistance"}{j \cdot DLL} \quad (23b)$$

has to be applied. Maximum load that can be achieved in the analysis' load increase is the load resistance. Its value is determined by a strength bound. This is performed by computing the modal *equivalent stresses* and the modal *stress efforts (Eff* $= \sigma_{eq} / R$*)* and by checking the remaining global stress effort reserve indicated by a value ≤ 1, **Fig. 14**. In the associated material-non-linear analysis the material's so-called IFF stress effort is kept constant when incrementally determining the changing stress state due to load redistribution versus the fibres.

No residual stresses are considered in the equations depicted in section5.3.

***Initial (IFF) Design Verification: Initial* failure load ≈ Design *Limit* Load**

Non-linear analysis considers hardening from non-linear stress-strain curves of the UD material, such as $\tau_{21}(\gamma_{21})$. Due to this material non-linearity, in spite of a proportional loading, IFF-related stresses increase less than proportional, **Fig. 15.** Proportional loading does not generate proportional stressing**.**

The afore-mentioned strength check during the incremental load increase provides the bound the computation may run up. The achieved load is the searched 'Initial failure load'. It is reached at that load when the stress effort becomes, see Eq.7b,

$$(Eff^{IFF})^{\dot{m}} = (Eff^{||\sigma})^{\dot{m}} + (Eff^{||\tau})^{\dot{m}} + (Eff^{\perp\sigma})^{\dot{m}} + (Eff^{\perp||})^{\dot{m}} + (Eff^{\perp\tau})^{\dot{m}} = 1. \quad (24)$$

***Final (FF) Design Verification: Final* failure load' ≥ Design *Ultimate* Load**

Now, material non-linear analysis has to consider hardening and softening (from intensive degradation of the embedded lamina; see *Figure 3* in [2]). *A*s practical limitation the load increase in the computation comes to its maximum value if the fibre strength $R_{f||}$ is reached in a single FF mode or in combination with the wedge mode IFF3, which means if

$$(Eff)^{\dot{m}} = (Eff^{||\sigma})^{\dot{m}} + (Eff^{||\tau})^{\dot{m}} + (Eff^{\perp\tau})^{\dot{m}} = 1. \quad (25)$$

The achieved load is the searched 'final failure load'. If numeric stops computation before reaching *Eff = 1* , then, it is also assumed that the final failure load is achieved. The successively computed *Eff value* is just a checking number not an accurate number as it will be the case for *Eff at 100%*.

5.4 Numerical Example for Design Verification

In this section a proposal for a *design verification* procedure is applied to a simple example: a bi-axial stress state in a point of a distinct lamina of a laminate. Input is:

* Load in the single dimensioning load case: DLL (*Design Limit Load = maximum expected load)*

* Critical stress state: $\{\sigma\}_L = (\varepsilon_1 \cdot E_{||}, \sigma_2, \tau_{21})^T = (+525, -74, +36)^T$ at DLL level

* IFF design curve: $F(\sigma_2, \tau_{21}, R_\perp^t, R_\perp^c, R_{\perp||}) = 1$, $B_{\perp||} = 0.6$, $\dot{m} = 3.1$

* Strength design allowables : $\{R\} = (R_{||}^t, R_{||}^c, R_\perp^t, R_\perp^c, R_{\perp||}) = (1050, 725, 27, 128, 54)^T$.

I Stress- based Resultant Reserve Factor Assumption: stress ~ load

For laminates, well-designed by netting theory (fibre net controls the strain behaviour) linear analysis is a good approximation on the safe side. In this case, the computation of the reserve factors is performed as follows:

$$f^{||\sigma} = \bar{R}_{||}^t / (\varepsilon_1 \cdot E_{||}) = 1050/525 = 2.0$$
$$f^{||\tau} = -2\bar{R}_{||}^c / (\sigma_1 - |\sigma_1|) = -725/0 ,$$
$$f^{\perp\sigma} = 2\bar{R}_\perp^t / (\sigma_2 + |\sigma_2|) = 27/0,$$
$$f^{\perp||} = (\bar{R}_{\perp||} - 0.5B_{\perp||} \cdot (\sigma_2 - |\sigma_2|))/|\tau_{21}| = 2.7,$$
$$f^{\perp\tau} = -2\bar{R}_\perp^c / (\sigma_2 - |\sigma_2|) = -128/-74 = 1.7 \leftrightarrow$$ design-driving mode = delamination-critical.

- Initial (IFF) Design Verification: $j = 1.0$!

Initial resultant reserve factor

$$(1/f_{Res}^{IFF})^{\dot{m}} = (j/f^{||\sigma})^{\dot{m}} + (j/f^{||\tau})^{\dot{m}} + (j/f^{\perp\sigma})^{\dot{m}} + (j/f^{\perp||})^{\dot{m}} + (j/f^{\perp\tau})^{\dot{m}}$$
$$= (j/2.0)^{\dot{m}} + (0)^{\dot{m}} + (0)^{\dot{m}} + (j/2.7)^{\dot{m}} + (j/1.7)^{\dot{m}}$$

$$\rightarrow f_{Res}^{IFF} = 1.41 \geq 1, \quad Eff^{IFF} = 1/f_{Res}^{IFF} = 0.71 \leq 1.$$

The design is accepted!

Stress results from non-linear analysis regarding hardening can be assessed in the same way.

- Final (FF) Design Verification*:* $j = j_{ult} = 1.25$

Final resultant reserve factor and final stress effort

$$(1/f_{Res}^{final})^{\dot{m}} = (j/f^{||\sigma})^{\dot{m}} + (j/f^{||\tau})^{\dot{m}} + (j/f^{\perp\sigma})^{\dot{m}} + (j/f^{\perp||})^{\dot{m}} + (j/f^{\perp\tau})^{\dot{m}}$$

$$\rightarrow f_{Res}^{final} = 1.14 \geq 1$$ or

$$(Eff)^{\dot{m}} = (j \cdot Eff^{||\sigma})^{\dot{m}} + (j \cdot Eff^{||\tau})^{\dot{m}} + (j \cdot Eff^{\perp\sigma})^{\dot{m}} + (j \cdot Eff^{\perp||}) + (j \cdot Eff^{\perp\tau})^{\dot{m}}$$

$$\rightarrow Eff = 0.88 = 1/f_{Res}^{final} \leq 1.$$

The design is accepted!

II Load-based Resultant Reserve Factor Assumption 'No residual stresses' -

Initial (IFF) Design Verification: $j = 1.0$ See stress-based case ! -

Final (FF) Design Verification: $j = j_{ult} = 1.25$ (chosen). $1/f_{Res} \neq Eff$ if non-linear

This case has to consider hardening, softening and geometrically non-linear effects. The equivalent stresses $\sigma_{eq}^{\perp\sigma}$ and $\sigma_{eq}^{\perp\|}$ degrade versus zero and $\sigma_{eq}^{\perp\tau}$ is considered hazardous in this application.

In parallel to the incremental loading, the stress effort has to be checked, **Fig. 16.** Highest load level reached in the computation was 1.51·DLL. After insertion of the associated lamina stresses calculated in the non-linear stress analysis (data assumed for this schematic procedure) the computed stress effort

$$(Eff)^{\dot{m}} = (Eff^{\|\sigma})^{\dot{m}} + (Eff^{\|\tau})^{\dot{m}} + (Eff^{\perp\tau})^{\dot{m}} \qquad \rightarrow \quad Eff = 0.95 \leq 1$$

was 95% <100% at reaching the highest computation level. Therefore, the final reserve factor

$$f_{Res}^{final} = \frac{1.51 \cdot DLL}{1.25 \cdot DLL} = 1.21 \geq 1.14 \geq 1$$

is larger than *1*. The design is accepted!

Note:
- The computed load capacity is higher than in the stress-based case.
- Probable residual stresses would have been vanished due to degradation.

6 Conclusions

The two objectives of this article are the development of numerically simple 3D/2D IFF conditions for UD laminae and the derivation of condition-associated reliable reserve factors necessary for the *design verification*. For both objectives the lessons learned are enlisted in the following:

* Mapping (fitting) of the courses of provided and own IFF test data by the new and simpler $F_{\perp\|}$ conditions is very good. In this context, with respect to accuracy we should keep in mind: There is a more or less large *scatter* in experiment, and we apply failure *models* to map the evaluated test data. As failure modelling is one subset of structural modelling one should not look for peanuts in failure modelling.

* Smeared modelling of a UD material which consists of fibres and matrix comes to its limit in the mode $F_{\|}^{\sigma}$. Here, failure occurs when the fibre strength $R_{f\|}$ is reached

* The full capacity of the fracture conditions could not be verified. There is still a need for generating reliable 2D test data not just for 3D data.

* The softening part of the stress-strain curve of an embedded (constraint) lamina is strain-controlled by the laminate [2]. As this ‘in-situ behaviour’ has not attracted much attention further work is highly recommended in order to achieve fully reliable reserve factor values.

* The determination of the lowest mode reserve factor as the design driving one is automatically given. The computation of the resultant reserve factor f_{Res} is integral part of the FMC procedure.

* Formulae for the determination of reserve factors in linear and non-linear cases are highlighted.

* In non-linear case the load has to be increased until its theoretical final failure is reached. This level is indicated by a stress effort $Eff = 100\%$ for the critical lamina in an analysis-accompanying check. The benefit of non-linear analysis on the reserve factor is outlined

* In non-linear analysis three effects have to be considered:
  - non-linear stress-strain behaviour of the smeared lamina material (hardening, below IFF),
  - beyond IFF, from degradation caused softening, and
  - non-linear geometrical behaviour including large strains and large deformations (had to be considered when applying some test cases of the WWFE which were not correctly evaluated)
* The mean curve is to be utilised in stress and deformation analysis
* For initial failure the application of linear analysis is sufficient in practice. In case of well-designed laminates, very often, linear analysis is sufficient even for final failure.

NOTE

Experiments and theory have a hand-in-hand relationship. Just well-understood experiments can verify the models. And, one has to keep in mind when considering the remaining gaps between theory and experiment: - Theory creates a model of the reality, 'only'
- An experiment is 'just' one realisation of the reality and experimental results can be far away from the reality like a bad theoretical model.

Acknowledgement:

The author gratefully thanks A. Freund for preparing the MATHCAD programme, and Prof. A. Puck for valuable comments.

References

[1] Cuntze RG, Freund A: The Predictive Capability of Failure Mode Concept-based Strength Criteria for Multidirectional Laminates. Part A. Composites Science and Technology 64 (2004), 343-377

[2] Cuntze RG. The Predictive Capability of Failure Mode Concept-based Strength Criteria for Multidirectional Laminates. Part B. Composites Science and Technology 63 (2004), 487-516

[3] Hinton MJ, Soden PD. Predicting failure in composite laminates: the background to the Exercise. Composites Science and Technology 58 (1998), 7, pp. 1001-1010

[4] Failure Criteria of fibre-reinforced-polymer Composites (summary of results of pre-runners, Part B of the Failure Exercise). Composites Science and Technology 62 (2002), 12-13, 1479-1797

[5] Hinton MJ, Kaddour AS, Soden PD. A Comparison of the Predictive Capabilities of Current Failure Theories for Composite Laminated, Judged against Experimental Evidence. Composite Science and Technology 62 (2002), 1725-1797

[6] Hinton MJ, Soden PD, Kaddour AS. Failure criteria in fibre reinforced polymer composites: The World-Wide Failure Exercise. Elsevier 2004 (ISBN: 0-08-044475-X), 700 pages

[7] Puck A, and Schürmann H. Failure Analysis of FRP Laminates by Means of Physically based Phenomenological Models. Composites Science and Technology 62 (2002), 1633-1662

[8] VDI 2014: German Guideline, sheet 3 'Development of FRP Components, Analysis'. (German and English. In press)

[9] Christensen RM. The Numbers of Elastic Properties and Failure Parameters for Fibre Composites. Transactions of the ASME, Vol. 120 (1998), 110-113

[10] Hashin Z. Failure Criteria for Unidirectional Fibre Composites. J. of Appl. Mech. 47 (1980), 329-334

[11] Boehler, J.P.: Failure Criteria for Glass-Fiber Reinforced Composites under Confining Pressure. *J. Struct. Mechanics 13 (1985), 371*

[12] Tsai SW, Wu EM. A General Theory of Strength for An-isotropic Materials. Journal Comp. Materials 5 (1971), 58-80

[13] Cuntze RG, Deska R, Szelinski B, Jeltsch-Fricker R, Meckbach S, Huybrechts D, Kopp J, Kroll L, Gollwitzer S, Rackwitz R. Neue Bruchkriterien und Festigkeitsnachweise für unidirektionalen Faserkunststoffverbund unter mehrachsiger Beanspruchung –Modellbildung und Experimente–. VDI-Fortschrittbericht, Reihe 5, Nr. 506 (1997), 250 pages. In German. (New fracture criteria (Hashin-Puck action plane criteria) and Strength Design Verifications' for Uni-directional FRPs subjected to Mult-iaxial States of Stress –Model development and experiments-)

[14] Paul, B. A modification of the Coulomb-Mohr Theory of Fracture. Journal of Appl. Mechanics 1961, p.259-268

[15]ECSS-E-30-02 Mechanical design, verification, qualification and acceptance of pressurised hardware. (final draft), ESA publications division, ESTEC, P.O. Box 299, 2200 AG Noordwijk, The Netherlands

ANNEX: MATHCAD programme used for mapping the courses of test data

The code was developed initially by A. Freund.

Input for the programme is the stress state $\{\sigma\} = (\sigma_1, \sigma_2, 0, 0, 0, \tau_{21})^T$.

Material parameters were taken from [13]: $bb_{sp} = 0.34$, $b_{\perp}^{\tau} = 1$ (not active), and see the input below

material parameters: $R_{pt} \equiv 1280$ $R_{pc} \equiv 800$ $R_{st} \equiv 55$ $R_{sc} \equiv 231$ $R_{sp} \equiv 97$ *in MPa* $B_{sp} \equiv 0.34$ $m° \equiv 2.$

test data set: $i := 0..70$ Test data points: $CFK_{i,0}$ $CFK_{i,1}$

loop: $k := 0..\frac{schluss - start}{inkr}$ $start \equiv -90$ $schluss \equiv 90$ $inkr \equiv 1$ $loadstep \equiv .5$ $stop \equiv 10000$

$TAU21_k := Lamina_{k,3}$ $SIG2_k := Lamina_{k,2}$

visualisation:

2D IFF2, Eq(13d)

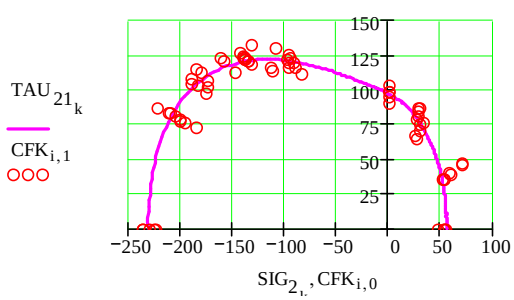

3D IFF2, Eq(4)

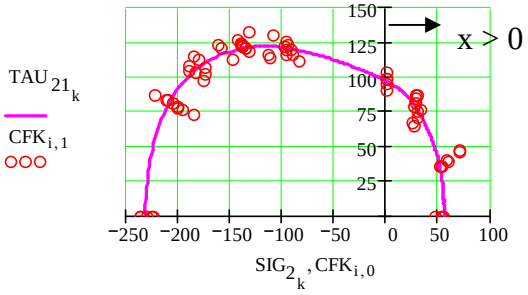

(Suffixes mean: p:=parallel || , s:= transversal or perpendicular ⊥)

Result: The graphs are practically identical for both $F_{\perp||}$ formulations.

The columns in the following MATHCAD programme represent the computation loops.

Lamina :=

$i \leftarrow 0$

for $x \in start, start + inkr .. schluss$

$l \leftarrow 0$

$end \leftarrow 0$

$ende \leftarrow stop + 1$

while $end < ende$

$l \leftarrow end$

$\sigma_1 \leftarrow l \cdot loadstep \cdot \cos(x \cdot Grad) \cdot SIG1$

$\sigma_2 \leftarrow l \cdot loadstep \cdot \cos(x \cdot Grad) \cdot SIG2$

$\tau_{21} \leftarrow l \cdot loadstep \cdot \sin(x \cdot Grad) \cdot TAU21$

$\sigma eq_{\sigma p} \leftarrow \left(\left|\sigma_1\right| + \sigma_1\right) \cdot 0.5$

$\sigma eq_{\tau p} \leftarrow \left(\sigma_1 - \left|\sigma_1\right|\right) \cdot -0.5$

$\sigma eq_{\sigma s} \leftarrow \left(\left|\sigma_2\right| + \sigma_2\right) \cdot 0.5$

$\sigma eq_{\tau s} \leftarrow \left(\sigma_2 - \left|\sigma_2\right|\right) \cdot -0.5$

$a \leftarrow \tau_{21}^{4} \cdot R_{sp}^{-4}$

$b \leftarrow 2 \cdot \left(\sigma_2 \cdot \tau_{21}^{2}\right) \cdot R_{sp}^{-3}$

$$\sigma eq_{sp} \leftarrow \begin{cases} 0 & \text{if } \tau_{21} < 0.01 \\ R_{sp}\sqrt{(2 \cdot a)} \cdot \left(-Bsp \cdot b + \sqrt{Bsp^{2} \cdot b^{2} + 4 \cdot a}\right)^{-0.5} & \text{otherwise} \end{cases}$$

$$Eff_{IFF} \leftarrow \left| \left[\left(\frac{\sigma eq_{\sigma s}}{R_{st}}\right)^{m^\circ} + \left(\frac{\sigma eq_{sp}}{R_{sp}}\right)^{m^\circ} + \left(\frac{\sigma eq_{\tau s}}{R_{sc}}\right)^{m^\circ} \right]^{\frac{1}{m^\circ}} \right|$$

$$Eff_{final} \leftarrow \left| \left[\left(\frac{\sigma eq_{\sigma p}}{R_{pt}}\right)^{m^\circ} + \left(\frac{\sigma eq_{\tau p}}{R_{pc}}\right)^{m^\circ} + \left(\frac{\sigma eq_{\tau s}}{R_{sc}}\right)^{m^\circ} \right]^{\frac{1}{m^\circ}} \right|$$

$$Eff_{res} \leftarrow \left| \left[\left[\left(\frac{\sigma eq_{\sigma p}}{R_{pt}}\right)^{m^\circ} + \left(\frac{\sigma eq_{\tau p}}{R_{pc}}\right)^{m^\circ} + \left(\frac{\sigma eq_{\sigma s}}{R_{st}}\right)^{m^\circ} + \left(\frac{\sigma eq_{sp}}{R_{sp}}\right)^{m^\circ} + \left(\frac{\sigma eq_{\tau s}}{R_{sc}}\right)^{m^\circ} \right] \right]^{\frac{1}{m^\circ}} \right|$$

$(end \leftarrow ende)$ if $Eff_{res} \geq 1$

$end \leftarrow end + 1$

$$Kurve^{\langle i \rangle} \leftarrow \left(x \;\; \sigma_1 \;\; \sigma_2 \;\; \tau_{21} \;\; \frac{\sigma eq_{\sigma s}}{R_{st}} \;\; \frac{\sigma eq_{\tau s}}{R_{sc}} \;\; \frac{\sigma eq_{sp}}{R_{sp}} \;\; Eff_{IFF} \;\; Eff_{final} \;\; Eff_{res} \right)^{T}$$

$i \leftarrow i + 1$

$((Kurve))^{T}$

3D

$\tau_{31} \leftarrow 0$

$\sigma_3 \leftarrow 0$

$\sigma eq_{\sigma p} \leftarrow \left(\left|\sigma_1\right| + \sigma_1\right) \cdot 0.5$

$\sigma eq_{\tau p} \leftarrow \left(\sigma_1 - \left|\sigma_1\right|\right) \cdot -0.5$

$\sigma eq_{\sigma s} \leftarrow \left[\left(\sigma_2 + \sigma_3\right) + \sqrt{\sigma_2^{2} - 2 \cdot \sigma_2 \cdot \sigma_3 + \sigma_3^{2}}\right] \cdot 0.5$

$\sigma eq_{\tau s} \leftarrow \left(bb_{s\tau} - 1\right) \cdot \left(\sigma_2 + \sigma_3\right) + bb_{s\tau} \sqrt{\sigma_2^{2} - 2 \cdot \sigma_2 \cdot \sigma_3 + \sigma_3^{2}}$

$$a \leftarrow \left[\frac{\left(\tau_{31}^{2} + \tau_{21}^{2}\right)}{R_{sp}^{2}}\right]^{2}$$

$$b \leftarrow 2 \cdot bb_{sp} \frac{\left(\sigma_2 \cdot \tau_{21}^{2} + \sigma_3 \cdot \tau_{31}^{2}\right)}{R_{sp}^{3}}$$

$$ba \leftarrow \frac{b}{2 \cdot a}$$

$$\sigma eq_{sp} \leftarrow \begin{cases} 0 & \text{if } \tau_{21} < 0.01 \\ R_{sp} \cdot \left(-ba + \sqrt{ba^{2} + \frac{1}{a}}\right)^{-0.5} & \text{otherwise} \end{cases}$$

Lamina =

	0	1	2	3	4	5	6	7	8	9	10
0	0	0	51	0	0	0	0	0	1	-0.27	0
1	10	0	50.23	8.86	0	0	0	0	0.98	-0.26	0.11
2	20	0	49.8	18.13	0	0	0	0	0.97	-0.26	0.22
3	30	0	48.5	28	0	0	0	0	0.95	-0.25	0.33
4	40	0	46.73	39.21	0	0	0	0	0.91	-0.24	0.46
5	50	0	42.42	50.56	0	0	0	0	0.83	-0.22	0.59
6	60	0	37	64.09	0	0	0	0	0.72	-0.19	0.74
7	70	0	28.39	77.99	0	0	0	0	0.55	-0.15	0.87
8	80	0	15.8	89.62	0	0	0	0	0.31	-0.08	0.96
9	90	0	-0	98	0	0	0	0	0	0	1
10	100	0	-18.23	103.4	0	0	0	0	0	-0.08	1
11	110	0	-40.02	109.94	0	0	0	0	0	-0.17	1
12	120	0	-67.5	116.91	0	0	0	0	0	-0.29	0.98
13	130	0	-103.49	123.33	0	0	0	0	0	-0.45	0.94
14	140	0	-146.31	122.77	0	0	0	0	0	-0.63	0.84
15	150	0	-187.06	108	0	0	0	0	0	-0.81	0.68
16	160	0	-214.25	77.98	0	0	0	0	0	-0.93	0.46
17	170	0	-227.49	40.11	0	0	0	0	0	-0.99	0.23
18	180	0	-231	-0	0	0	0	0	0	-1	0
19											

Table of analysis data: 3D condition

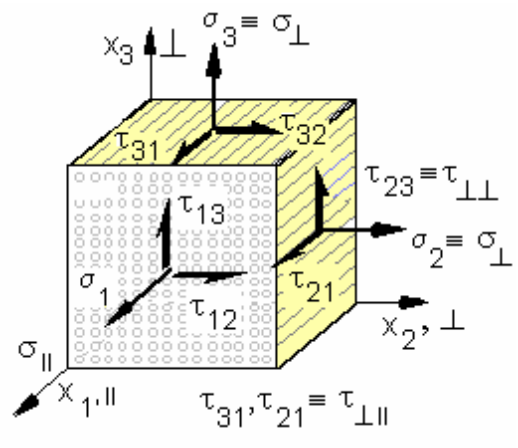

Fig. 1. Stresses, invariants, and strength notations of a UD lamina element. [VDI 2014 guideline]
t: = tension, c: = compression, f := index fibre.

$R_{\parallel}^{t}\,(=X^{t}),\ R_{\parallel}^{c}\,(=X^{c}),\ R_{\perp\parallel}\,(=S),\ R_{\perp}^{t}\,(=Y^{t}),\ R_{\perp}^{c}\,(=Y^{c})$;

$E_{\parallel}, E_{\perp}, G_{\parallel\perp}, \nu_{\perp\parallel}, \nu_{\perp\perp}$;

$\{\sigma\}=(\sigma_1,\sigma_2,\sigma_3,\tau_{23},\tau_{13},\tau_{12})^T$.

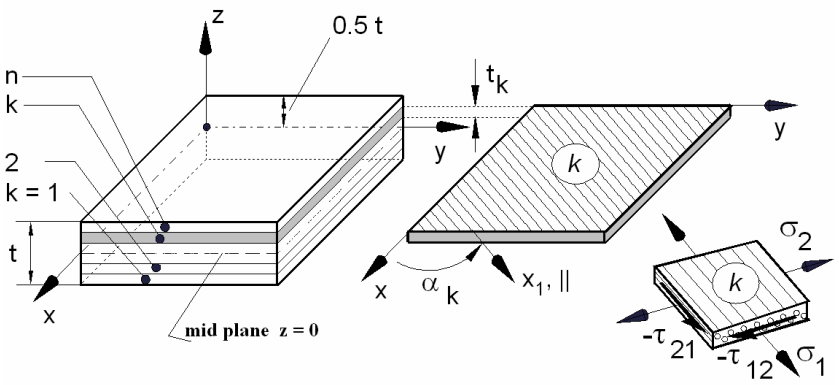

Fig 2. Laminate and k' th lamina subjected to a plane state of stress (mid-plane z = 0).

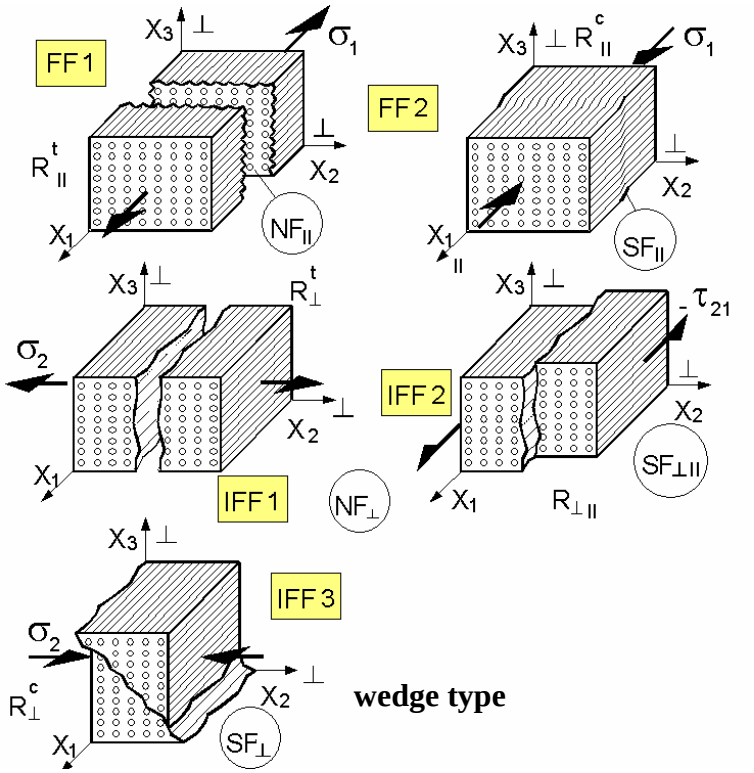

Fig.3. Fracture modes (types) in transversally-isotropic material.
NF:= Normal Fracture,
SF:= Shear Fracture. [13]

Fig. 4. IFF features in isolated and embedded laminae (for $F_{\perp\|}$ similar)

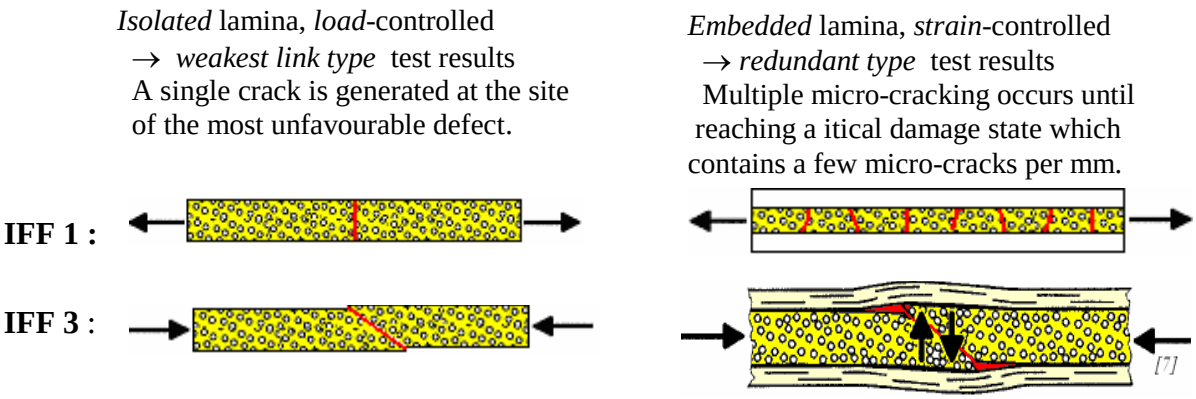

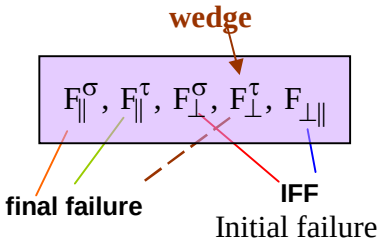

Fig. 5. Failure mode criticality

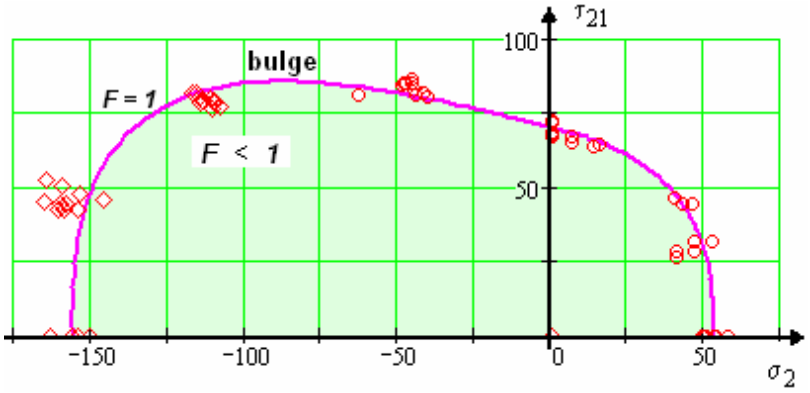

Fig. 6. $\tau_{21}(\sigma_2)$ course of test data, hoop wound tubes[13]. E-glass/LY556/HT976.

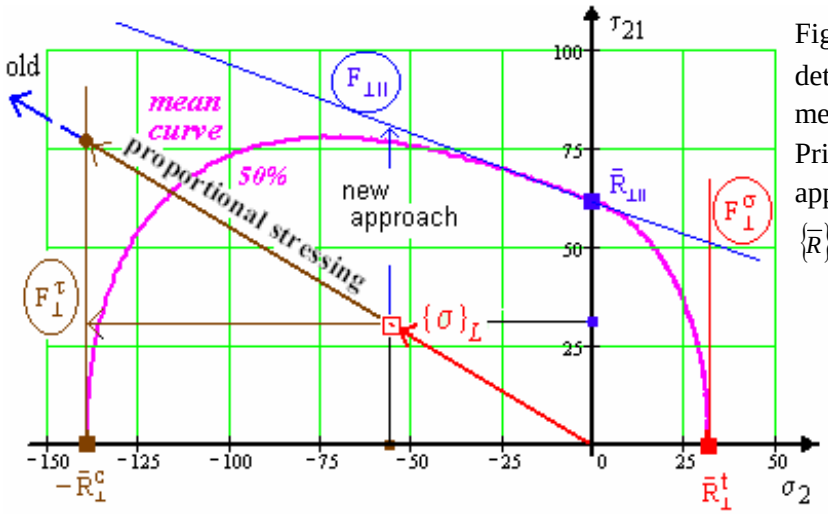

Fig. 7. Mean curve $F(\sigma_i, \bar{R}_i) = 1$ derivation with determination of mode stretch factors in case of mechanical load-stresses $\{\sigma\}_L = j \cdot \{\sigma(DLL)\}$. Principle of proportional stressing (old) and new approach for $F_{\perp\|}$.
$\{\bar{R}\}$=(1140, 570, 34, 135, 62)^T .

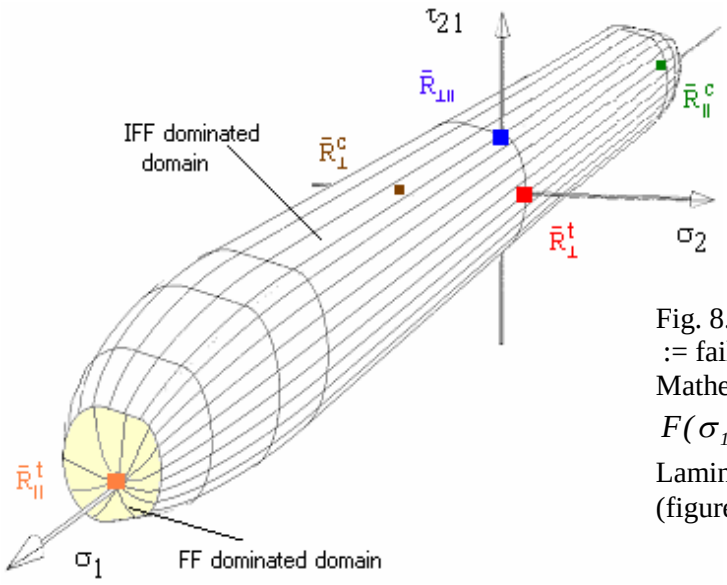

Fig. 8. The 2D failure body or failure surface := failure limit state, termed fracture cigar. Mathematically described by Eq(14), $F(\sigma_1,\sigma_2,\tau_{21},\bar{R}_{||}^{t},\bar{R}_{||}^{c},\bar{R}_{\perp}^{t},\bar{R}_{\perp}^{c},\bar{R}_{\perp||})=1$. Lamina strengths depicted (figure after VDI 2014, Huybrechts)

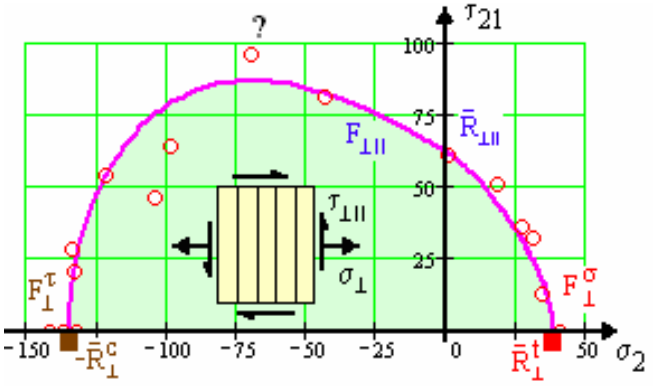

Fig. 9. $\tau_{21}(\sigma_2)$ 3D IFF curve, hoop wound tubes. Test case 1 in WWFE. GFRP: E-Glass/LY556 epoxy. $\{\bar{R}\}=(1140,\ 570,\ 38,\ 135,\ 62)^T$.

$bb_{\perp||}$=1.1, $\dot{m}$=2.0 , Eq(4 and 7a)

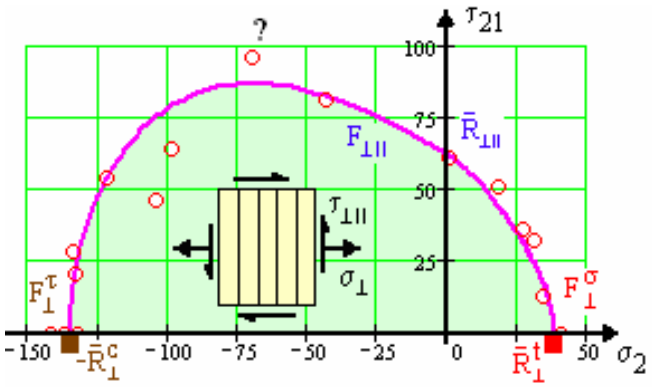

Fig. 10. 2D-reduced 3D condition $\tau_{21}(\sigma_2)$ IFF curve, hoop wound tubes. Test case 1 in WWFE [2] GFRP: E-Glass/LY556 epoxy. $\{\bar{R}\}=(1140,\ 570,\ 38,\ 135,\ 62)^T$,

$B_{\perp||}$=1.1, $\dot{m}$=2.0 . Eqs(14)

$$\left(\frac{\sigma_2}{\bar{R}_{\perp}^{t}}\right)^{\dot{m}}+\left(\frac{\tau_{21}}{\bar{R}_{\perp||}-B_{\perp||}\cdot\sigma_2}\right)^{\dot{m}}+\left(\frac{-\sigma_2}{\bar{R}_{\perp}^{c}}\right)^{\dot{m}}=1\,.$$

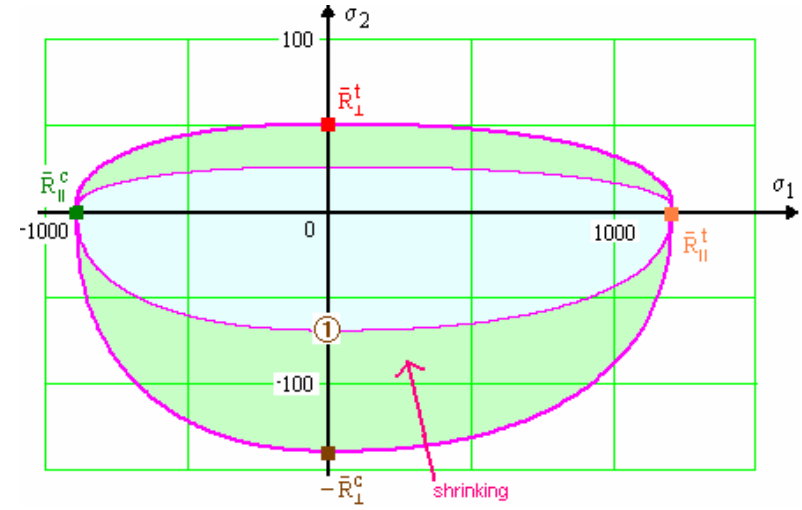

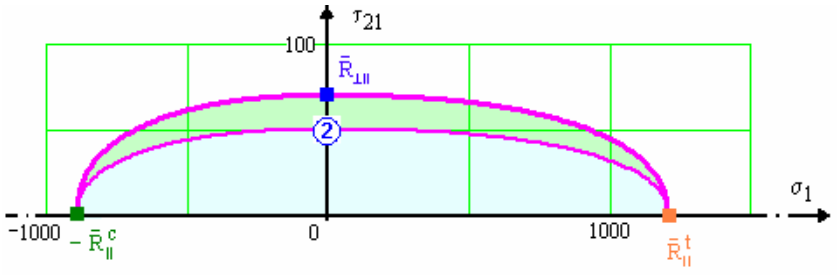

Fig. 11. Main sections $\tau_{21}(\sigma_2)$ and $\sigma_2(\sigma_1)$ of the 2D failure body, originally and after shrinking due to a distinct IFF degradation. Eq.(15a)

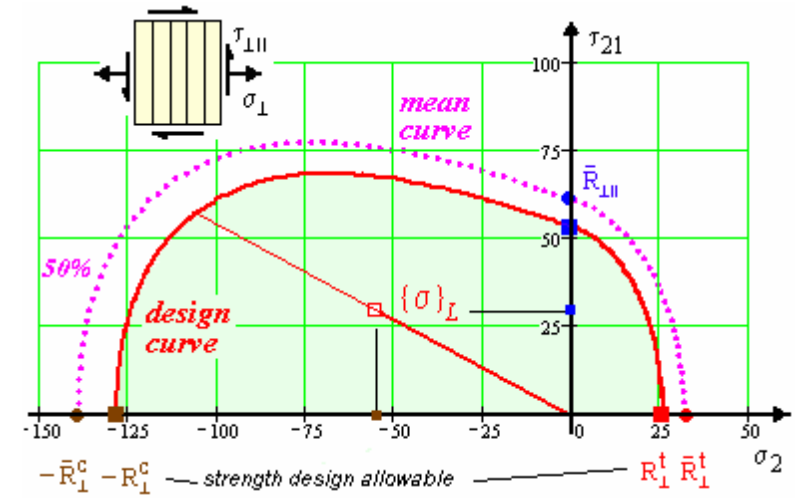

Fig. 12. Design curve with determination of a stress-based reserve factor in case of load-stresses.

Mean curve: $F(\sigma_i, \bar{R}_i) = 1$.

$\{\bar{R}\}$=*(1140, 570, 34, 135, 62)*^{T} , $B_{\perp\parallel}$= *0.6* .

- Design curve: $F(\sigma_i, R_i) = 1$.

$\{R\}$=*(1050, 525, 27, 128, 54)*^{T} , $B_{\perp\parallel}$= *0.6* .

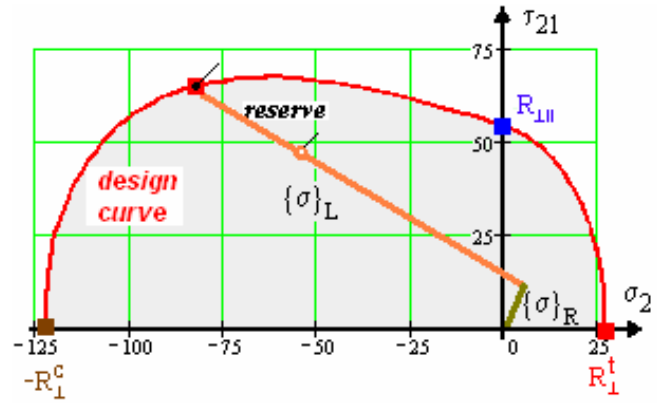

Fig. 13. Determination of a stress-based reserve factor in case of load stresses acting together with residual stresses.

Design curve: $F(\sigma_i, R_i) = 1$.

$\{R\}$ = $(R_{\parallel}^{t}, R_{\parallel}^{c}, R_{\perp}^{t}, R_{\perp}^{c}, R_{\perp\parallel})$

= *(1050, 725, 27, 128, 54)*^{T}

$\{\sigma\}_L = j \cdot \{\sigma(DLL)\}$.

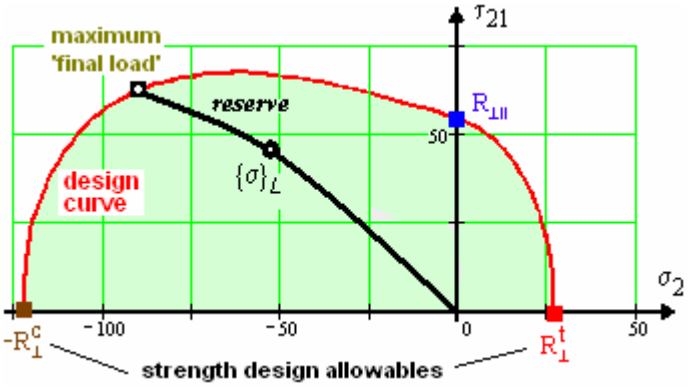

Fig. 14. Determination of reserve factor in non-linear case.

$\{R\} = (R^t_{\parallel}, R^c_{\parallel}, R^t_{\perp}, R^c_{\perp}, R_{\perp\parallel})$

$= (1050, 725, 27, 128, 54)^T$

$\{\sigma\}_L = \sigma(j \cdot DLL)$

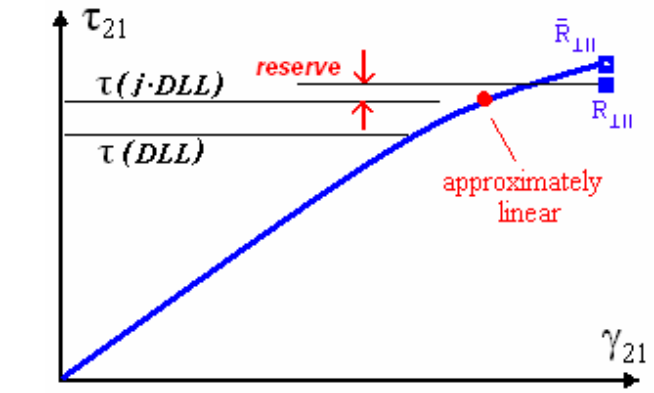

Fig. 15. Reasons for permitting linear analysis, visualised for $\tau_{21}(\gamma_{21})$

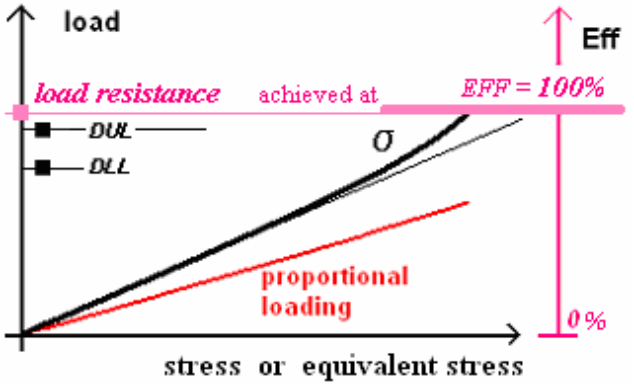

Fig.16. Non-linear case: Visualisation of non-proportionality of load increase and stress increase

Table 1 Main features of the FMC [1]

• According to the symmetry of a transversally-isotropic material there are 5 strengths, 5 elasticity quantities and therefore, the FMC postulates 5 failure modes • Each *mode* represents one theoretically independent failure mechanism and one piece of the complete *failure surface* • Each failure *mechanism* is represented by one failure *condition*. One failure mechanism is governed by one basic strength and therefore has a clearly defined equivalent stress σ_{eq} • Invariant formulations [11] of the failure conditions in order to achieve a *scalar* potential considering the material's symmetries are derivable for each mode. Each invariant term in the failure condition is related to one mechanism observed, causing a volume change or a shape change in the material element • Curve-fitting of the course of test data is only permitted in the pure failure mode regimes • For each *mode* one associated *reserve factor* f_{Res}^{mode} is to be determined. The lowest (highest risk) mode reserve factor displays, where the design key has to be turned • A probabilistic-based 'rounding-off' approach automatically provides the global *reserve factor* f_{Res} necessary for achieving the *design verification.*

Table 2 System of strength failure domains for a transversally-isotropic non-porous UD material
SY:=shear yielding, NF:=normal fracture caused by σ^t, SF:=shear fracture

$\Rightarrow$ **onset of yielding**	**Yielding**	$\Rightarrow$ **onset of fracture**	**Fracture**	
	SY		**NF**	**SF**
	F_y		$F_{\parallel}^{\sigma}$, $F_{\perp}^{\sigma}$ (tension)	$F_{\parallel}^{\tau}$, $F_{\perp}^{\tau}$, $F_{\perp\parallel}$